Stem Cells Translational Medicine, 2022, **11**, 659–673
https://doi.org/10.1093/stcltm/szac025
Advance access publication 1 June 2022
Original Research

Periostin Attenuates Cyclophosphamide-induced Bladder Injury by Promoting Urothelial Stem Cell Proliferation and Macrophage Polarization

Zhihong Chen[‡,2,3], Liyong Liu[‡,1,2], Yunhua Chen[4,‡], Minjie Liu[2], Andy Peng Xiang[1,2], Chunhua Deng[*,3], Mei Hua Jiang[*,1,2,5,6]

[1]Program of Stem Cells and Regenerative Medicine, Affiliated Guangzhou Women and Children's Hospital, Zhongshan School of Medicine, Sun Yat-sen University, Guangzhou, Guangdong, People's Republic of China
[2]Center for Stem Cell Biology and Tissue Engineering, Key Laboratory for Stem Cells and Tissue Engineering, Ministry of Education, Sun Yat-sen University, Guangzhou, Guangdong, People's Republic of China
[3]Department of Andrology, The First Affiliated Hospital, Sun Yat-sen University, Guangzhou, Guangdong, People's Republic of China
[4]National Engineering Research Center for Tissue Restoration and Reconstruction, School of Materials Science and Engineering, South China University of Technology, Guangzhou, Guangdong, People's Republic of China
[5]Department of Anatomy, Zhongshan School of Medicine, Sun Yat-sen University, Guangzhou, Guangdong, People's Republic of China
[6]Guangdong Key Laboratory of Reproductive Medicine, Guangzhou, Guangdong, People's Republic of China

*Corresponding authors: Mei Hua Jiang, Department of Anatomy, Zhongshan School of Medicine, Sun Yat-sen University, Guangzhou 510080, People's Republic of China. Tel: +86 20 87330639; Fax: +86 20 87330709; Email: jiangmh2@mail.sysu.edu.cn; or, Chunhua Deng, Department of Andrology, The First Affiliated Hospital, Sun Yat-sen University, Guangzhou 510080, People's Republic of China. Tel: +86 20 87335633; Fax: +86 20 87332200; Email: dengchh@mail.sysu.edu.cn
‡These authors contributed equally and share the first authorship.

Abstract

Interstitial cystitis (IC) is a bladder syndrome of unclear etiology with no generally accepted treatment. Growing evidence suggest that periostin (POSTN) is an important homeostatic component in the tissue repair and regeneration in adulthood, but its function in urinary bladder regeneration is still unknown. Here we investigate whether POSTN is involved in bladder tissue repair in a cyclophosphamide (CYP)-induced interstitial cystitis model. POSTN is primarily expressed in bladder stroma (detrusor smooth muscle and lamina propria) and upregulated in response to CYP-induced injury. POSTN deficiency resulted in more severe hematuria, aggravated edema of the bladder, and delayed umbrella cell recovery. Besides, less proliferative urothelial cells (labeled by pHH3, Ki67, and EdU) and lower expression of Krt14 (a urothelial stem cell marker) were detected in *POSTN*$^{-/-}$ mice post CYP exposure, indicating a limited urothelial regeneration. Further investigations revealed that POSTN could induce Wnt4 upregulation and activate AKT signaling, which together activates β-catenin signaling to drive urothelial stem cell proliferation. In addition, POSTN can promote resident macrophage proliferation and polarization to a pro-regenerative (M2) phenotype, which favors urothelial regeneration. Furthermore, we generated injectable P-GelMA granular hydrogel as a biomaterial carrier to deliver recombinant POSTN into the bladder, which could increase urothelial stem cells number, decrease umbrella cells exfoliation, and hence alleviate hematuria in a CYP-induced interstitial cystitis model. In summary, our findings identify a pivotal role of POSTN in bladder urothelial regeneration and suggest that intravesical biomaterials-assisted POSTN delivery may be an efficacious treatment for interstitial cystitis.

Key words: periostin; urothelial regeneration; cystitis; macrophage polarization; biomaterials.

Received: 7 November 2021; Accepted: 27 March 2022.

Graphical Abstract

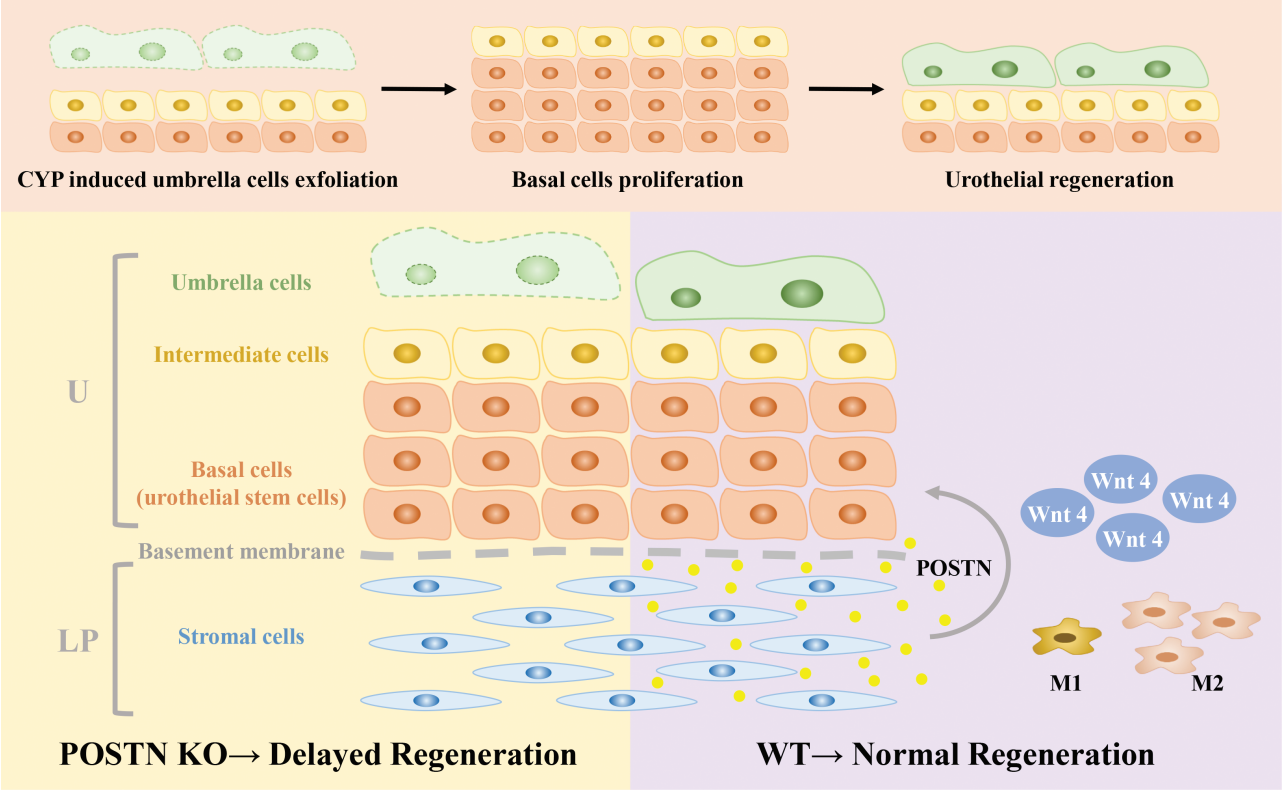

Abbreviations: bHLH: transcription factor; BMP4: bone morphogenetic protein 4; CCND1: cyclin D1; Cdh-1: E-cadherin; c-Myc: MYC proto-oncogene, bHLH transcription facto; CYP: cyclophosphamide; Krt14: keratin 14; Krt20: keratin 20; Krt5: keratin 5; OCLN: occludin; POSTN: periostin; SHH: sonic hedgehog signaling molecule; Upk3a: uroplakin 3A; USCs: urothelial stem cells; ZO-1: zonula occludens-1.

Significance Statement

Interstitial cystitis (IC) severely affects patients' quality of life worldwide, and biomaterial-assisted drug delivery is considered as a promising strategy for IC treatment. Herein, we verified that periostin (POSTN) could promote urothelial regeneration and thus alleviate hematuria in CYP-induced interstitial cystitis animal model. In addition, we produced injectable P-GelMA granular hydrogel as a biomaterial carrier to assist intravesical POSTN delivery, which significantly accelerated urothelial regeneration and reestablished the bladder barrier. This study highlights POSTN as a promising bioactive molecule in urothelial regeneration and bladder diseases.

Introduction

Interstitial cystitis, also known as a bladder pain syndrome (IC/BPS), is clinically characterized by pelvic pain, urinary frequency, and urgency, which causes severe adverse effects on a patient's quality of life.[1] It has been reported that a large population of more than 10 million citizens in the US (3-7% in women and 2-4% in men) suffered from IC/BPS.[2] Available treatments for IC are still limited and low efficacious. For example, oral administration of pentosan polysulfate sodium (PPS) was approved and recommended by FDA for IC/BPS treatment, as it helped to restore the injured glycosaminoglycan (GAG) layer which covers the umbrella cells and contributes to urothelial barrier function. However, a recent multicenter, double-blind, randomized, placebo-controlled study revealed no therapeutic effect of PPS for IC/BPS compared to placebo.[3] Therefore, it is important to explore a simple and direct treatment to restore bladder function and alleviate symptoms of IC.

Recent studies have proved bladder epithelial alteration as a key role in the development of IC.[4] Disruption of the urothelial barrier is closely associated with interstitial cystitis as well as bladder carcinoma.[5] The multi-layered bladder epithelium forms an impermeable bladder barrier to separate the urinary space and prevent harmful substances and pathogens from the underlying tissue, in which luminal umbrella cells are mainly responsible for maintaining the barrier by expression of uroplakin plaques and intercellular junction proteins (including tight junctions as well as adherence junctions).[6-8] Under homeostatic conditions, the urothelium is quiescent and has a slow turnover rate. However, it arises a rapid proliferation of urothelial stem cells (USCs) in response to injury and complete restoration of newly differentiated umbrella cells within three days.[9-11] Abnormalities of urothelial proliferation lead to urinary bladder diseases, most notably chemical or bacterial-induced cystitis, and bladder carcinoma. Therefore, mechanisms underlying bladder urothelial regeneration have been a key scientific problem. Kunyoo Shin et al. put forward a urothelium–mesenchyme crosstalk pattern in bladder re-epithelium in response to injury, in which a Hedgehog/Wnt signaling feedback loop supports the proliferation of basal cells or urothelium stem cells.[12]

Nevertheless, mechanisms of urothelial regeneration have not yet been fully understood and need further elucidation.

The matricellular protein periostin (POSTN) has been identified in several tissues during embryonic development and is known to support the continuous repair and regeneration of tissues in an adult body.[13-16] Current evidence reveal that the expression of POSTN is transiently increased in response to insults in many tissues, and deficiency of POSTN will delay the process of tissue regeneration, such as bone, liver, pancreas, and kidney.[15,17,18] Through binding to integrin receptors, POSTN promotes cell adhesion, migration, and proliferation, which enhances tissue regeneration in physiological or pathological conditions. Besides, POSTN has been reported to recruit and promote resident macrophage proliferation as well as polarization to M2-subtype macrophage, which favors wound healing and tissue regeneration.[19,20] As mentioned above, POSTN is a potential tissue repair molecule, but it's unknown whether POSTN contributes to bladder urothelial regeneration.

In this study, we used a cyclophosphamide (CYP)-induced acute cystitis mouse model to investigate the possible role of POSTN in bladder urothelial regeneration. We demonstrated that POSTN was expressed in the bladder under physiological conditions and strongly upregulated in response to injury. POSTN deficient mice showed worsened bladder structure and impaired urothelial regeneration post–CYP exposure. Further studies showed POSTN promoted urothelial stem cells proliferation and urothelial regeneration via the AKT/β-catenin pathway. Besides, POSTN drove resident macrophage proliferation and polarization into a pro-regenerative M2 phenotype. Moreover, we developed a novel strategy, namely intravesical delivery of P-GelMA granular hydrogel–loaded recombinant POSTN, to attenuate CYP-induced bladder injury. Taken together, our results show that POSTN plays a pivotal role in promoting bladder urothelial regeneration, and could be a promising therapeutic target for interstitial cystitis.

Materials and Methods

Animals

All animal protocols were reviewed and approved by the Sun Yat-sen University Institutional Animal Care and Use Committee. Heterozygous B6;129-Postn^{tm1Jmo1}/J *(POSTN*$^{+/-}$) mice were purchased from the Jackson Laboratory (Bar Harbor, Maine, USA) and crossed with wild–type C57BL/6J mice for over ten generations to generate *POSTN*$^{+/-}$ mice in a C57BL/6J background. POSTN knockout *(POSTN*$^{-/-}$) and wild–type mice were generated by crossing *POSTN*$^{+/-}$ mice with *POSTN*$^{+/-}$ mice. All mice used for in vivo studies were 12-week-old female mice with a bodyweight of 25-30 g, and mice were randomly allocated to each group. Mice were maintained in a specific pathogen-free facility.

Cyclophosphamide-induced Acute Cystitis Mouse Model

The mouse model of acute cystitis was induced by cyclophosphamide (CYP). A single dose of 150 mg/kg CYP (Macklin, CN) was administered intraperitoneally as previously described.[21-23] On days 1, 3, and 7 post–CYP administration, wild-type, and *POSTN*$^{-/-}$ mice were sacrificed and bladders were harvested.

Synthesis of Injectable P-GelMA Granular Hydrogel

Gelatin methacryloyl (GelMA) and fluorescein isothiocyanate (FITC) tagged GelMA were firstly prepared according to the methods described in previous literature.[24-26] GelMA (0.8 g) was dissolved in 10 mL deionized water at 45 °C, and 0.016 g of potassium persulfate (KPS) was added under gentle stirring. The solution was degassed with nitrogen for 30 min, then 30 μL of *N,N,N′,N′*-tetramethylethylenediamine (TEMED) was added. The polymerization was allowed to proceed overnight at 45 °C. The obtained hydrogel was dialyzed against deionized water for 5 days, and then sheared with ultra-turrax at 25 000 rpm for 2 min. The granular particles were then lyophilized and stored at –20 °C before use. The injectable hydrogel with a solid concentration of 6 wt% was obtained by dispersing the granular particles in deionized water.

Characterization of P-GelMA Granular Hydrogel

The morphology of granular particles was observed using an inverted fluorescence microscope (Leica, Germany). The rheological tests were conducted on an Anton Paar MCR 302 rheometer (Anton Paar, GmbH). A stainless parallel plate with a diameter of 8 mm (PP-08) was employed in the measurements of moduli under the oscillation mode. Granular hydrogel (300 μL) was injected into the gap at 25 °C. To prevent water evaporation, the gap was sealed with silicone oil. For amplitude sweep tests, the oscillation mode was employed at 37 °C. The strain was swept from 0.1% to 100% logarithmically. For internal morphology characterization, the P-GelMA granular hydrogel was quickly frozen by immersing in liquid nitrogen and lyophilized. The fracture surface of the lyophilized samples was observed using an FEI Q25 scanning electron microscope under 5.0 kV acceleration voltage after platinum sputtering.

Intravesical Administration of P-GelMA Granular Hydrogel–Loaded Recombinant POSTN

Recombinant POSTN was added to the PBS or P-GelMA granular hydrogel at a final concentration of 1 ug/mL. Immediately after CYP treatment, an equal volume of 50 uL POSTN, P-GelMA, or P-GelMA–loaded with POSTN were respectively delivered to the empty bladder through a catheter, and kept with a retention time of 5 min before removing the instillation catheter. Mice were sacrificed on days 1 and 3 post-CYP exposure and bladders were harvested for further analysis.

RNA Isolation, Reverse Transcription, and Quantitative Real-time PCR (qRT-PCR)

Total RNA was extracted from cell lysates and bladder tissues using TRIzol reagent (Invitrogen), and 1 μg of RNA was reverse transcribed using a RevertAid first-strand cDNA synthesis kit (Thermo Scientific, Waltham, MA, USA). qRT-PCR was performed using the SYBR Green qRT-PCR SuperMix (Roche) and detected by a Light Cycler 480 Detection System (Roche). The relative mRNA abundance was calculated using the ΔCt or ΔΔCt methods, and each targeted mRNA level was normalized with respect to that of GAPDH. The sequences of primers used in this study are listed in Supplementary Table S1.

Western Blot Analysis

The bladders were dissected, and the urothelial layer was mechanically separated with fine forceps under a transillumination dissection microscope. Total proteins were extracted from urothelium lysates, and the protein concentration was measured using a bicinchoninic acid (BCA) protein assay kit (Thermo Scientific). Equal amounts of proteins were separated by 8% sulfate-polyacrylamide gel electrophoresis and transferred to a polyvinylidene fluoride (PVDF) membrane. The membrane was blocked with Tris-buffered saline with Tween 20 (TBS/T) containing 5% nonfat dry milk and incubated with primary antibodies listed in Supplementary Table S2. The results were confirmed by at least 3 independent experiments.

Histological Analysis

At indicated days post–CYP treatment, bladders were collected, fixed, and further processed for immunofluorescence staining. Briefly, the bladders were fixed with 4% PFA, dehydrated in 30% sucrose, and further embedded in OCT compound (Sakura Finetek, Japan), and sectioned at a thickness of 5 μm. Bladder sections were blocked with normal goat serum for 40 min and then incubated with primary antibodies overnight at 4 °C, followed by incubation with secondary antibodies (1:500 dilution) to protect from the light at room temperature for 1 h. Nuclei were visualized with 4′,6-diamidino-2-phenylindole (DAPI, Sigma–Aldrich). The primary and secondary antibodies used are listed in Supplementary Table S2. Negative controls were prepared by substituting PBS for the primary antibody. All images were obtained using an LSM-780/800/880 confocal microscope (Zeiss, Heidenheim, Germany). For quantitative cell analysis, 5 random fields per section and at least 3 sections from independent experiments are counted in each group.

Labeling Cell Proliferation with Click-it EdU In Vivo

To characterize the proliferative response of urothelium, EdU (50 mg/kg; Thermo Scientific, USA) was injected (i.p.) daily for 3 consecutive days following CYP injection. The mice were sacrificed 1 day after the final injection of EdU, and the bladder sections were stained with Click-it®EdU cell Fluor Cell Proliferation Assay Kit (Invitrogen, USA) according to the manufacturer's instruments; nuclei were counterstained with DAPI.

Statistics

All results were performed in at least 3 independent experiments and expressed as mean ± SEM. Comparisons of means between 2 groups were performed using Student's *t*-test, while comparisons of 3 or more groups were made by one-way ANOVA followed by a *t*-test corrected for multiple comparisons. $P < .05$ was considered significant. Analysis and graphs were performed using GraphPad Prism software 8.03 (San Diego, CA, USA).

Results

Periostin Expression in the Bladder of Mice Treated with CYP

To detect the expression and localization of POSTN in the urinary bladder, we used immunofluorescent staining for POSTN in bladder sections of wild-type and *POSTN*$^{-/-}$ mice. As shown in Fig. 1A, we found POSTN mainly located in laminate propria and smooth muscle, rather than in urothelium of bladder from wild–type mice, while no immunostaining was detected in bladder section from negative control and *POSTN*$^{-/-}$mice.

To elucidate whether matricellular protein POSTN has a role in bladder urothelial regeneration, the expression of POSTN was monitored by qRT-PCR in bladder specimens from CYP–treated mice. The result showed that the expression of POSTN was significantly elevated in the bladder in response to injury, peaked on day 1, and gradually returned to baseline on day 7 post–CYP treatment (Fig. 1B). A similar tendency was observed in the POSTN protein level detected by Western blot (Fig. 1C). As a comparison, POSTN was not detected in bladders of *POSTN*$^{-/-}$ mice by qRT-PCR and Western blot (Fig. 1B, 1C). Taken together, these results showed POSTN was upregulated in bladders in response to CYP-induced injury, indicating a possible role of POSTN in bladder regeneration.

Periostin Deficiency Deteriorates Bladder Structure and Function Following CYP Treatment

To explore the effects of POSTN in the bladder, we used a transgenic global POSTN knockout mouse model (*POSTN*$^{-/-}$) for further experiments. Wild-type and *POSTN*$^{-/-}$ mice received an equal dose of CYP injection, and bladders were harvested for further analysis on day1, 3, and 7 post-CYP treatment (Fig. 2A). No obvious changes were observed in morphology and histology of bladders between wild-type and *POSTN*$^{-/-}$ mice under physiological conditions (Fig. 2B, left panel and 2E, left panel). However, after CYP treatment, bladders of *POSTN*$^{-/-}$ mice showed more severe edema extremely on days 1 and 3. In accordance, compared with wild–type mice, *POSTN*$^{-/-}$ mice exhibited a significantly higher bladder/bodyweight ratio on days 1 and 3 after CYP treatment, indicating more severe edema of the bladder (Fig. 2D). H&E staining showed moderate suburothelial edema, umbrella cell exfoliation, and inflammatory cells infiltration on day 1 and a complete recovery on day 7 in the bladder of wild–type mice post–CYP treatment. In contrast, POSTN deficiency resulted in more severe edema, umbrella cells exfoliation, and inflammatory cells infiltration, as well as delayed recovery (Fig. 2E).

Hematuria is often used to evaluate the severity of CYP-induced bladder injury and disruption of the blood–urine barrier. Therefore, sporadic urine was collected on days 0, 1, 3, 7 post–CYP treatment from all mice, and immediately observed and quantified under a microscope. The number of urine red blood cells increased and peaked on day 1 post-injury in both groups, but POSTN deficiency caused much more severe hematuria on day 1, implying worsening disruption of the blood–urine barrier in *POSTN*$^{-/-}$ mice (Fig. 2F). Taken together, these results showed that POSTN deficiency deteriorates CYP-induced bladder injury.

Periostin is Required for Bladder Barrier Repair in CYP-Treated Mice

As is reported, cyclophosphamide is converted into acrolein in the urine and then causes toxic damage to superficial umbrella cells and triggers urothelial regeneration. Hence, Krt20 immunohistochemical staining was performed to trace the loss and regeneration of umbrella cells (Fig. 3A). CYP treatment caused umbrella cells damage and exfoliation on day

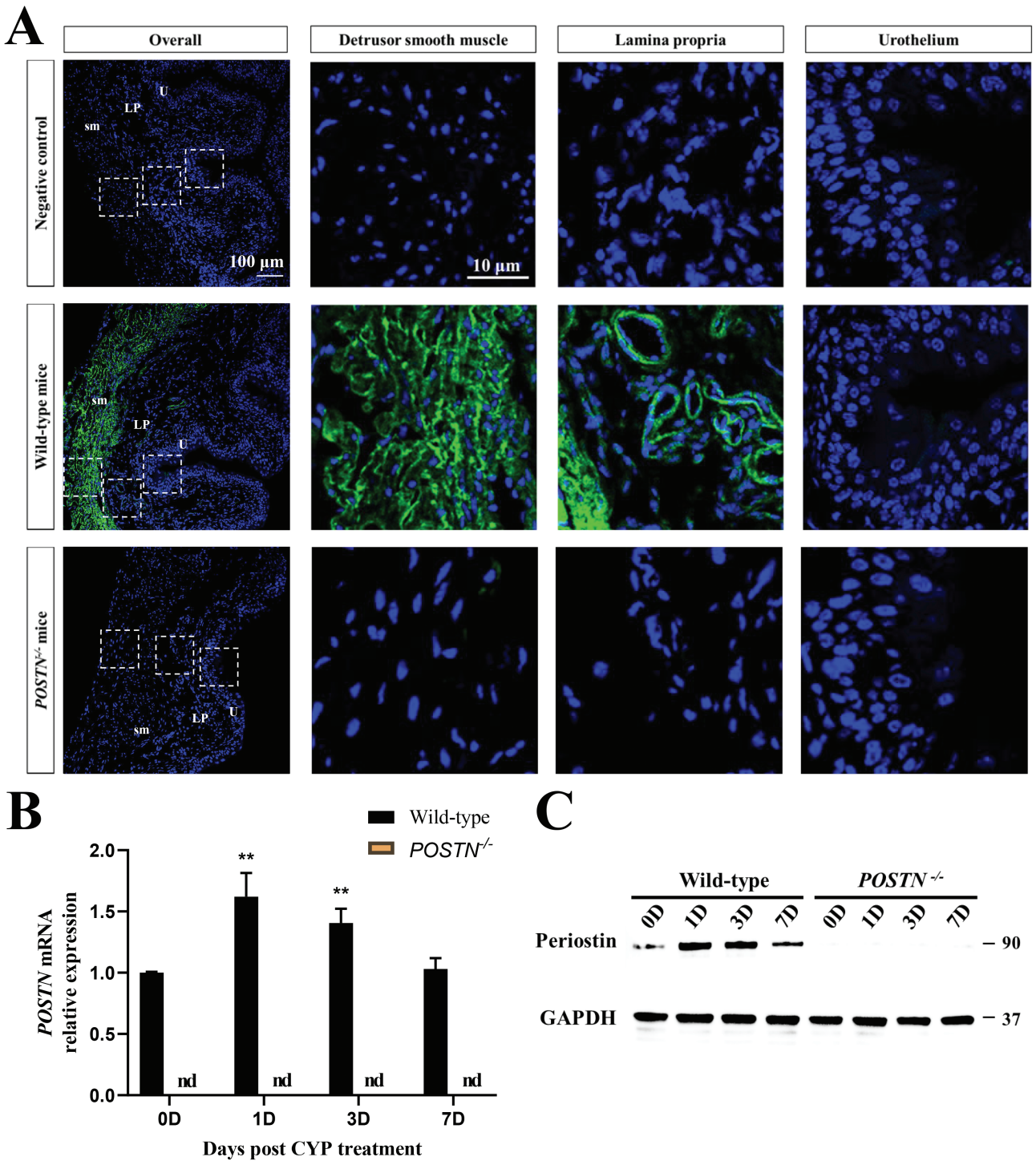

Figure 1. Expression of Periostin in the bladder. (**A**) Immunofluorescent staining for POSTN (green) was detected in bladders of wild-type and *POSTN*$^{-/-}$ mice. Scale bar, 100 μm and 10 μm. L, lumen; U, urothelium; LP, lamina propria; sm, detrusor smooth muscle. (**B**) The qRT-PCR analysis showed that the expression of POSTN in bladders at indicated days (0, 1, 3, 7 days post–CYP treatment). Data were represented as mean ± SEM of $n = 6$. Unpaired Student's *t*-test, $^{*}P < .05$, and $^{**}P < .01$, *POSTN*$^{-/-}$ group versus wild–type group. Nd, not detected. (**C**) The protein expression levels of POSTN in bladders were determined by Western blot.

1 in both groups. However, new-generated umbrella cells rapidly lined the luminal bladder and re-established the urothelial barrier at day 3 in wild–type mice, while incontinence of umbrella cells was still observed in *POSTN*$^{-/-}$ mice. Co-staining for UpkIIIa (a marker of umbrella cells) and Krt5 (a marker of basal cells) also revealed a complete recovery of umbrella cells 3 days post–CYP treatment, whereas a partial recovery in *POSTN*$^{-/-}$ mice. Besides, we performed qRT-PCR to detect markers of umbrella cells, and the heatmap showed that expression of uroplakins (including *Upk1a*, *Upk1b*, *Upk2*, *Upk3a*, and *Upk3b*) was first declined on day 1 and upregulated as the urothelial regeneration at day 3 in wild–type mice, whereas uroplakins remained low expression level and upregulated until day 7 in *POSTN*$^{-/-}$ mice (Fig. 3B).

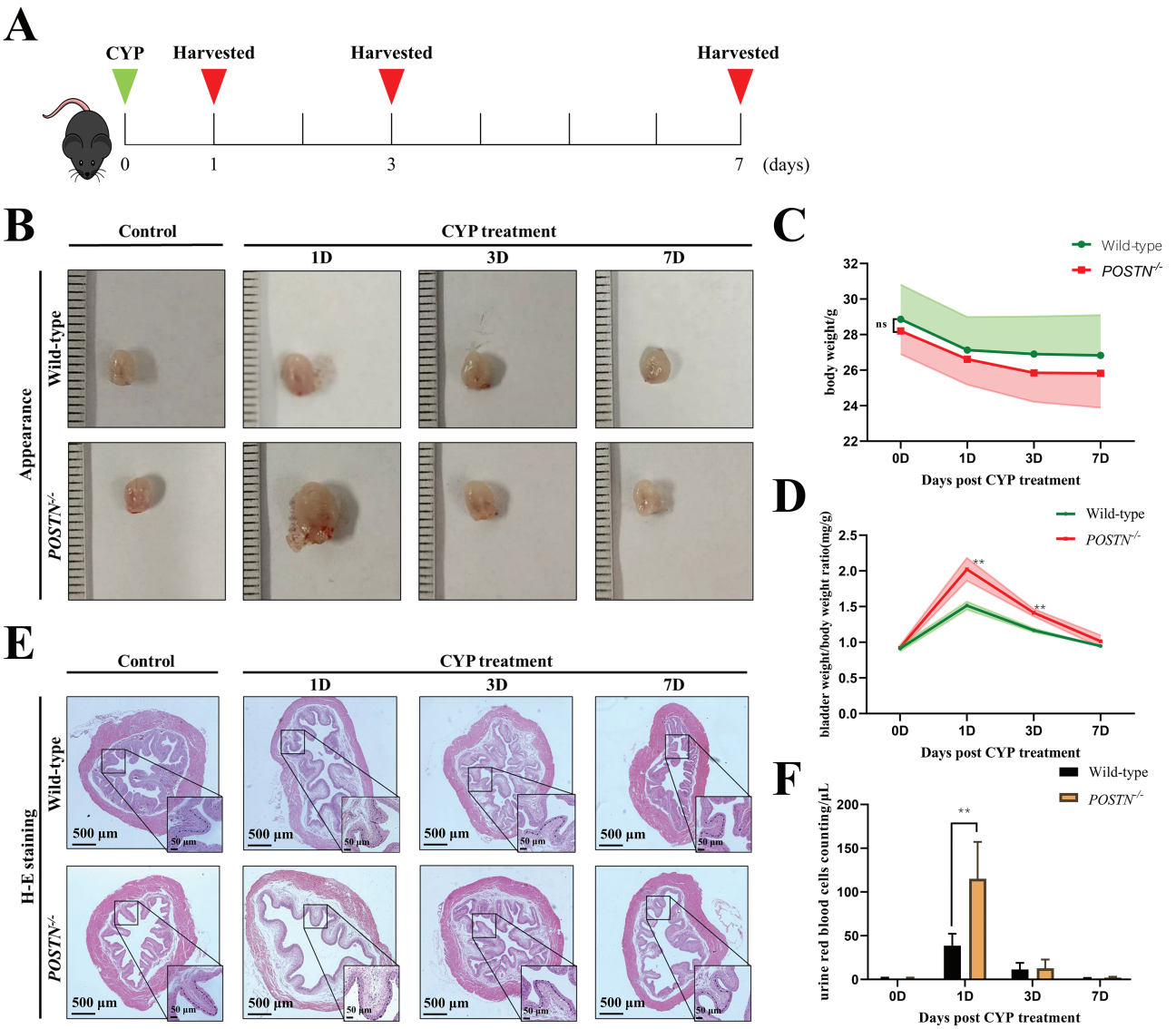

Figure 2. Periostin deficiency prolonged the altered bladder structure and function observed in CYP-treated mice. (**A**) Schematic depiction of the animal experimental procedure. (**B**) Macroscopic view of CYP–treated bladders in wild-type and *POSTN*$^{-/-}$ mice at indicated days (0, 1, 3, 7 days post–CYP treatment). (**C**–**D**) Bodyweight curves (C) and bladder/bodyweight ratio (D) were assessed in wild-type and *POSTN*$^{-/-}$ mice after CYP treatment ($n = 6$ in each group). (**E**) Representative images show H&E staining of bladder cross-sections in each group. Dotted lines indicate the superficial–intermediate cell boundary. (**F**) The number of urine red blood cells was counted in both groups on the indicated days after CYP treatment ($n = 6$ in each group). All data were represented as mean ± SEM of $n = 6$. Unpaired Student's *t*-test, $^{*}P < .05$, and $^{**}P < .01$, *POSTN*$^{-/-}$ group versus wild–type group.

Consistent with mRNA levels, UpkIIIa showed a similar protein expression pattern detected by Western blot (Fig. 3D). In addition to uroplakins, tight junction and adherence proteins are also essential for umbrella cells to form the urothelial barrier, such as tight junctional protein zonula occludens-1 (encoded by *ZO-1*), occludin (encoded by *OCLN*), and E-cadherin (encoded by *Cdh-1*). Compared to wild–type mice, expression levels of *ZO-1*, *OCLN* and *Cdh-1* were significantly lower in the bladders of *POSTN*$^{-/-}$ mice after CYP treatment (Fig. 3E). In summary, mice lacking POSTN showed a delayed umbrella cells regeneration and impaired bladder barrier repair in response to insult.

Periostin Drives Urothelial Proliferation via AKT/β-catenin Pathway

Previous studies have demonstrated that urothelium undergoes rapid repair and regeneration in response to acute injury, characterized by local proliferation of basal cells and differentiation into superficial umbrella cells. We thereby examined the expression of proliferation markers, pHH3 and Ki67, by immunofluorescence staining (Fig. 4A, 4B). We observed that pHH3 or Ki67 positive urothelial cells in wild–type mice increased rapidly on day 1 and peaked on day 3 post–CYP treatment. However, POSTN depletion dramatically haltered the proliferative response of urothelium, in which much fewer pHH3 or Ki67 positive cells were observed in *POSTN*$^{-/-}$ mice (Fig. 4A, 4B, 4C, 4D). Similarly, mRNA expression of the proliferative markers *Mki67* and *Aukrb* increased up to 80 and 60-fold, respectively in wild–type mice 3 days after CYP treatment, whereas fewer increase folds were detected in POSTN deficient mice (Fig. 4E, 4F). To further trace the regenerative process, we applied EdU to label new-generated urothelial cells within 3 days post-injury (Fig. 4G). In the trace of

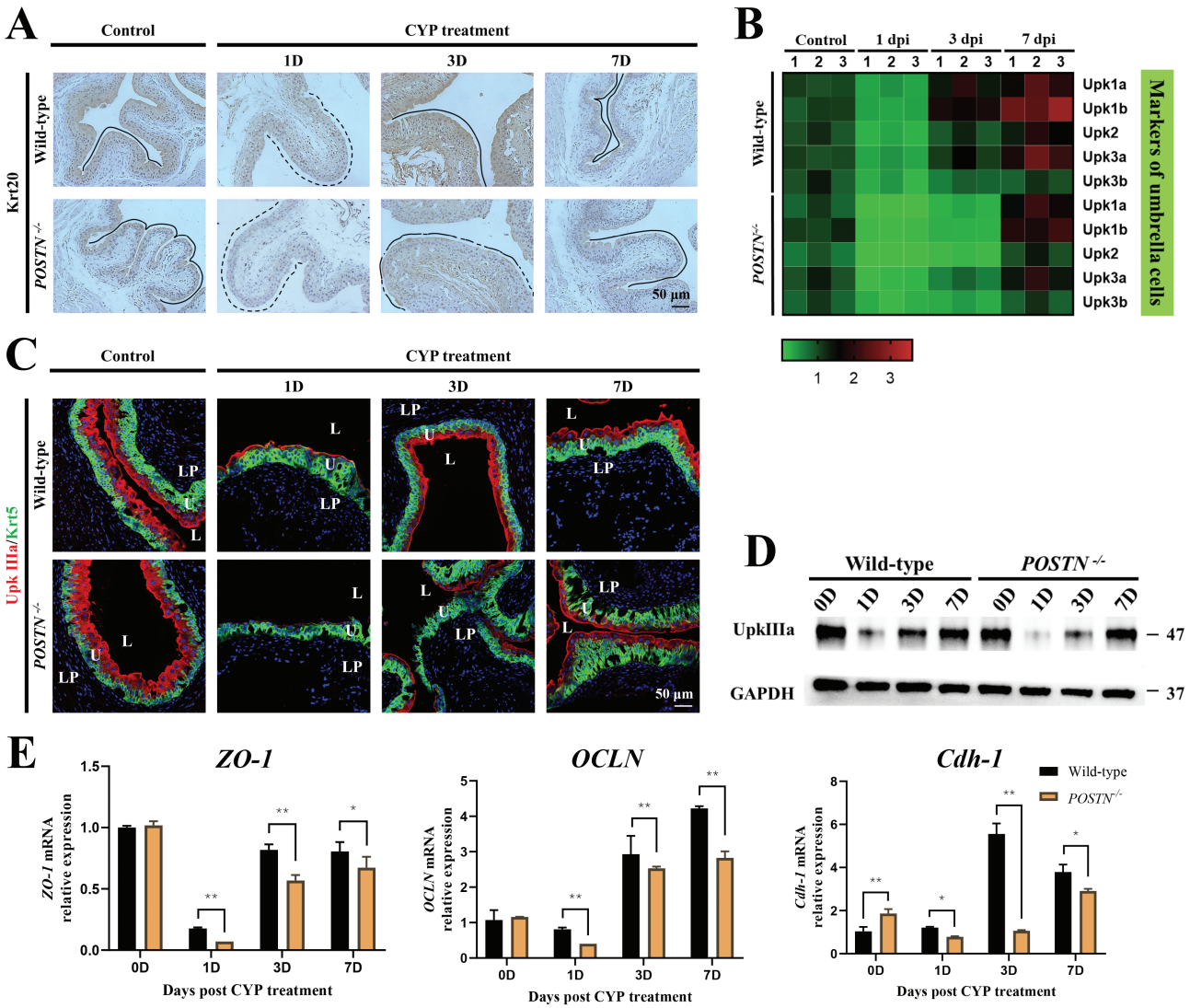

Figure 3. Periostin deficiency delayed the recovery of umbrella cells post–CYP treatment. (**A**) Immunohistochemical staining for Krt20 (a marker of umbrella cells) in bladder cross-sections of wild-type and *POSTN*$^{-/-}$ mice at indicated days post–CYP treatment. Solid and dotted lines indicate the presence and loss of superficial umbrella cells, respectively. Scale bar, 50 μm. (**B**) Heat map depiction of umbrella cells related genes in bladders of wild-type and *POSTN*$^{-/-}$mice (n = 3 in each group). (**C**) Co-staining for UpkIIIa (a marker of umbrella cells) and Krt5 (a marker of basal cells) in bladder cross-sections of wild-type and *POSTN*$^{-/-}$ mice at indicated days post–CYP treatment. Scale bar, 50 μm. (**D**) The protein expression levels of UpkIIIa in bladders were determined by Western blot. (**E**) The qRT-PCR analysis of tight junction markers (*ZO-1, OCLN*) and adherence marker (*Cdh-1*) in CYP–treated bladders of both groups. Data were represented as mean ± SEM of n = 6. Unpaired Student's t-test, *P < .05, and **P < .01, *POSTN*$^{-/-}$ group versus wild–type group.

the proliferative response of urothelium, EdU was injected daily for 3 consecutive days following CYP injection. Immunofluorescence staining revealed a higher number of new-generated Krt5^{+}/EdU^{+} basal cells and UpkIIIa^{+}/EdU^{+} umbrella cells in wild–type mice than that in *POSTN*$^{-/-}$ mice, implying POSTN promotes basal cells proliferation and differentiation into umbrella cells (Fig. 4G, 4H). What's more, Western blot showed that POSTN deficiency haltered the increased expression of Krt14 (a marker of urothelial stem cells) in response to CYP-induced bladder injury (Fig. 4I). Immunofluorescent images also showed a fewer number of Krt14 positive urothelial stem cells in *POSTN*$^{-/-}$ mice (Fig. 4J, 4K).

The above results indicate an important role of POSTN in urothelial regeneration and bladder repair via activating basal cells or urothelial stem cells proliferation and differentiation into umbrella cells, in which the underlying mechanisms need to be further studied. Since Wnt/β-catenin signaling is well acknowledged as a key regulator in urothelial regeneration, we detected the mRNA expression of Wnt ligands in bladders, including *Wnt1*, *Wnt2*, *Wnt2b*, *Wnt3*, *Wnt3a*, *Wnt4*, *Wnt5a*, *Wnt5b*, *Wnt7a*, *Wnt8b, and Wnt9b* (Fig. 5A, 5B). We found a significant increase of Wnt4 expression in the mRNA and protein levels of the bladder 1 day post–CYP administration in wild–type mice (Fig. 5C, 5D), and expression levels of AKT and β-catenin were hence elevated and peaked at day 3 by Western blot (Fig. 5E). Besides, nuclear translocation of β-catenin was observed and mainly co-expressed with EdU-incorporating urothelial cells, indicating activation of wnt/β-catenin signaling and subsequent induction of related genes (*c-Myc*, *CCND1*, and *AXIN2*) (Fig. 5F). However, POSTN deficiency inhibited Wnt4 upregulation in the bladder and

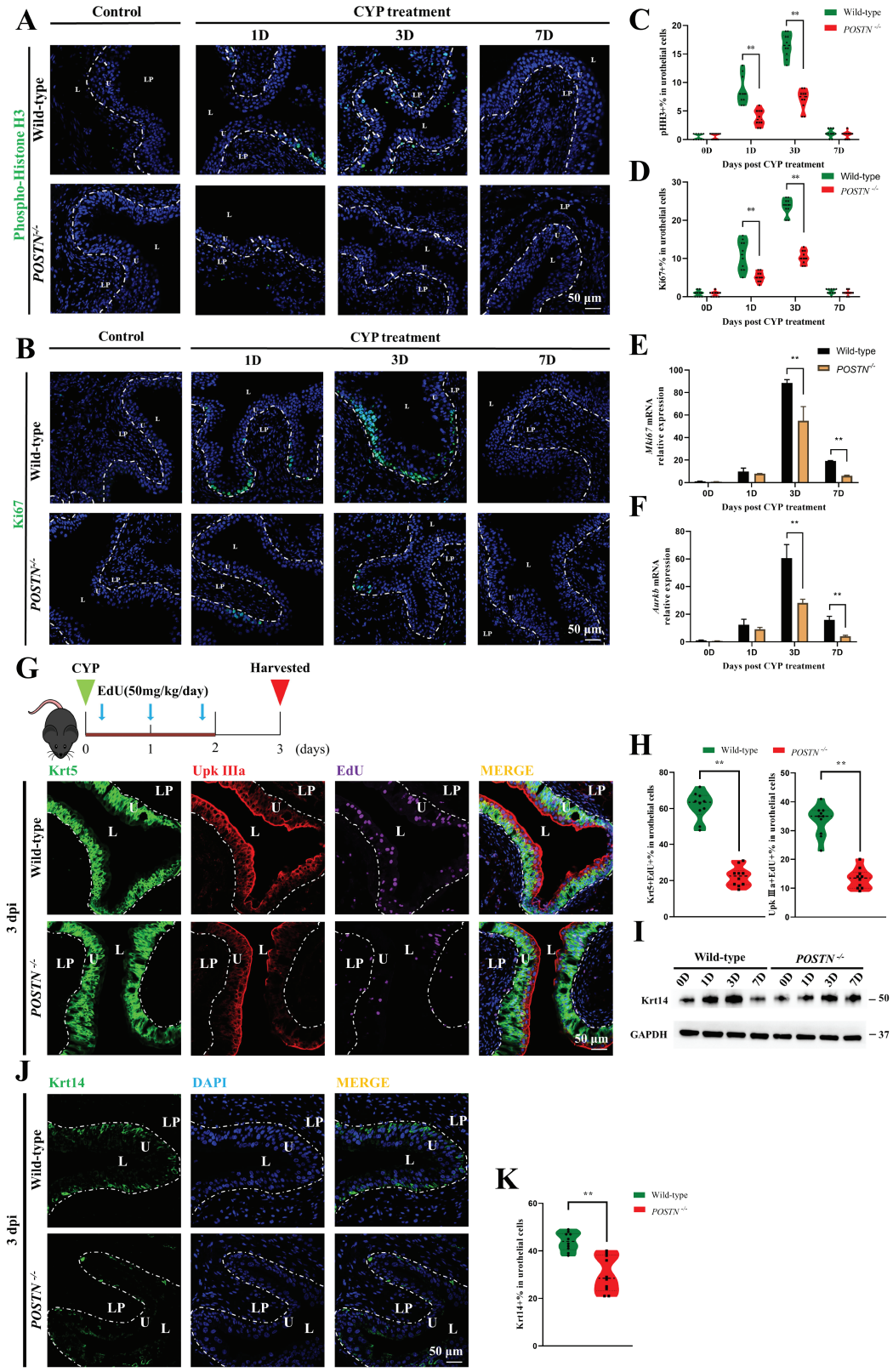

Figure 4. Periostin promotes urothelial proliferation in response to CYP–induced injury. (**A-B**) Representative images showed immunofluorescent staining for proliferative markers (pHH3 and Ki67) in bladder cross-sections of wild-type and *POSTN*$^{-/-}$ mice at indicated days post–CYP treatment. Dotted lines indicate the basement between the urothelium and lamina propria. Scale bar, 50 μm. (**C-D**) Quantitative analysis showing the percentage of pHH3 or Ki67 positive cells in urothelium of both groups. Three representative areas per slide were randomly selected from 6 independent animals. (**E-F**) The qRT-PCR analysis showed that the expression of *Mki67* and *Aurk* in bladders of wild-type and *POSTN*$^{-/-}$ mice at indicated days (0, 1, 3, 7 days post–CYP treatment). (**G**) Immediately after CYP administration, mice received EdU i.p. injection daily for 3 consecutive days, and bladders were harvested 1 day after the last EdU injection. Representative images showing new-generated basal cells stained for Krt5 (green) and EdU (purple), as well as new–generated umbrella cells stained for UpkIIIa (red) and EdU (purple). Scale bar, 50 μm. (**H**) Quantitative analysis shows the percentage

thus diminished activation of β-catenin signaling. Taken together, POSTN promotes urothelial cell proliferation via induction of Wnt4 and AKT and hence activation of β-catenin signaling.

Periostin Induces Resident Macrophage Proliferation and Polarization to M2-subtype

Resident macrophage has an essential role in tissue injury and regeneration, and POSTN can regulate macrophage proliferation and polarization.[15] CD68$^+$ pan-macrophages were less abundant at the repair phase of CYP–injured bladder in POSTN deficient mice (Fig. 6A). This decline was associated with the lower proliferation of CD206$^+$ resident macrophages in the *POSTN*$^{-/-}$ mice, detected by co-staining with proliferative marker EdU. Interestingly, although a lower expression level of CD68 was detected by qRT-PCR in *POSTN*$^{-/-}$ mice, a higher expression of *CD86* (an M1 marker) and lower CD206 (an M2 marker) were also assessed compared to wild–type mice (Fig. 6B). To further confirm whether POSTN affects macrophages polarization, we labeled macrophage with F4/80 and CD206 in the bladder 3 days post-injury. As expected, POSTN deficiency resulted in a decreased proportion of F4/80$^+$/CD206$^+$ M2-subtype in F4/80$^+$ pan-macrophage, implying decreased M2 polarization (Fig. 6D, 6E). Consequently, M2 macrophage secreted pro-regenerative cytokines such as *IL-4* and *IL-10* were much less in POSTN KO mice (Fig. 6C). In summary, POSTN promotes bladder resident macrophage proliferation and polarization to the M2-subtype, which provides a pro-regenerative microenvironment in response to acute injury.

Intravesical Administration of P-GelMA Granular Hydrogel–Loaded Recombinant POSTN Promotes Urothelial Regeneration

Intravesical biomaterials-assisted drug delivery for interstitial cystitis has gained more and more attention recently, as biomaterial carriers can prevent premature drug release by urine and prolong the drug residence time.[27] Therefore, we produced granular particles by mechanically shearing GelMA hydrogel. As shown in Supplementary Fig. S1A, the average diameter of particles is approximately 43 μm. Supplementary Fig. S1B shows the strain sweep measurement of the granular hydrogel. It is clear that the storage modulus (G′) is dominated in the strains ranging from 0.1% to 10%, indicating the gelling state of the hydrogel formulation. After increasing the applied strains, the value of G′ decreases dramatically. A crossover occurs above the strain of 10%, suggesting the interaction between granular particles breaks and the hydrogel turns into a sol state. This shear-thinning feature is essential for designing injectable hydrogels. The injectability of this granular hydrogel was confirmed by the smooth injection from a syringe (Supplementary Fig. S1C). The hydrogel porosity was characterized by SEM analysis, as shown in Supplementary Fig. S1D, abundant interconnect pores were distributed in the hydrogel after lyophilized, which might be beneficial for the diffusion of oxygen and nutrients, facilitating cell growth and migration.

Next, we dissolved recombinant POSTN in P-GelMA granular hydrogel and injected it into the bladders via a catheter immediately after CYP treatment (Fig. 7A). We found intravesical administration of P-GelMA–loaded POSTN, rather than recombinant POSTN or P-GelMA alone, could alleviate edema and weight of bladder 1 day after CYP treatment (Fig. 7B, 7D). Besides, sporadic urine was collected from all groups and urine red blood cells were counted under a microscope. CYP treatment caused hematuria most severely on day 1 and this could be attenuated by intravesical administration of P-GelMA–loaded POSTN rather than POSTN or P-GelMA alone (Fig. 7C). H&E staining further revealed less umbrella cell exfoliation after P-GelMA–loaded POSTN treatment (Fig. 7E), which was also confirmed by immunostaining for UpkIIIa (Fig. 7F). P-GelMA–loaded POSTN also increased the number of urothelial stem cells labeled by Krt14, indicating a more active urothelial regeneration. Taken together, intravesical administration of P-GelMA–loaded POSTN could promote urothelial regeneration and prevent bladder barrier injury from CYP treatment.

Discussion

In the present study, we demonstrate a pivotal role of POSTN in bladder urothelial regeneration in response to cyclophosphamide-induced injury. Using a global POSTN knockout transgenic strain, we show for the first time that POSTN promotes bladder urothelial regeneration after CYP treatment at least by 2 mechanisms: (1) POSTN drives basal cells or urothelial stem cells proliferation and replaces damaged umbrella cells by induction of Wnt4/AKT/β-catenin signaling, and (2) POSTN promotes resident macrophage proliferation and polarization into a pro-regenerative phenotype, thus favoring urothelial regeneration.

Previous studies revealed that the expression of POSTN will be transiently increased in various tissues in response to injuries or inflammatory stimulation, and a high level of POSTN is essential for tissue regeneration, including bone, heart, liver, kidney, and pancreas.[15,17,28-30] As an extracellular matrix molecule, POSTN might remodel the tissue microenvironment to generate a supportive niche for tissue regeneration by altering the levels of cytokines, conditioning the matrix, and/or remodeling the cell-matrix interactions.[17] However, the role of POSTN in the bladder has not yet been investigated. Here, we found that POSTN was upregulated first and decreased gradually in the bladder of CYP treated mice in both the mRNA and protein levels, suggesting a possible role in bladder regeneration.

Under normal conditions, bladder urothelium has a very low turnover rate,[10,17] and the lifespan of rodent umbrella cells is approximately 200 days.[31,32] However, the urothelium undergoes rapid proliferation and generates new superficial umbrella cells in response to acute injuries caused by chemicals like cyclophosphamide, bacterial infection, mechanical overdistention, subtotal cystectomy, etc.[10,33-37]

of Krt5/EdU and UpkIIIa/EdU double-positive cells in the urothelium of both groups. (**I**) The protein expression levels of Krt14 (a marker of urothelial stem cell) in bladders were determined by Western blot. All data were represented as mean ± SEM. Unpaired Student's *t*-test, **P* < .05, and ***P* < .01, *POSTN*$^{-/-}$ group versus wild–type group. (J) Immunostaining shows Krt14 labeled urothelial stem cells 3 days post–CYP injection. (**K**) Quantitative analysis shows the percentage of Krt14 positive cells in the urothelium of both groups.

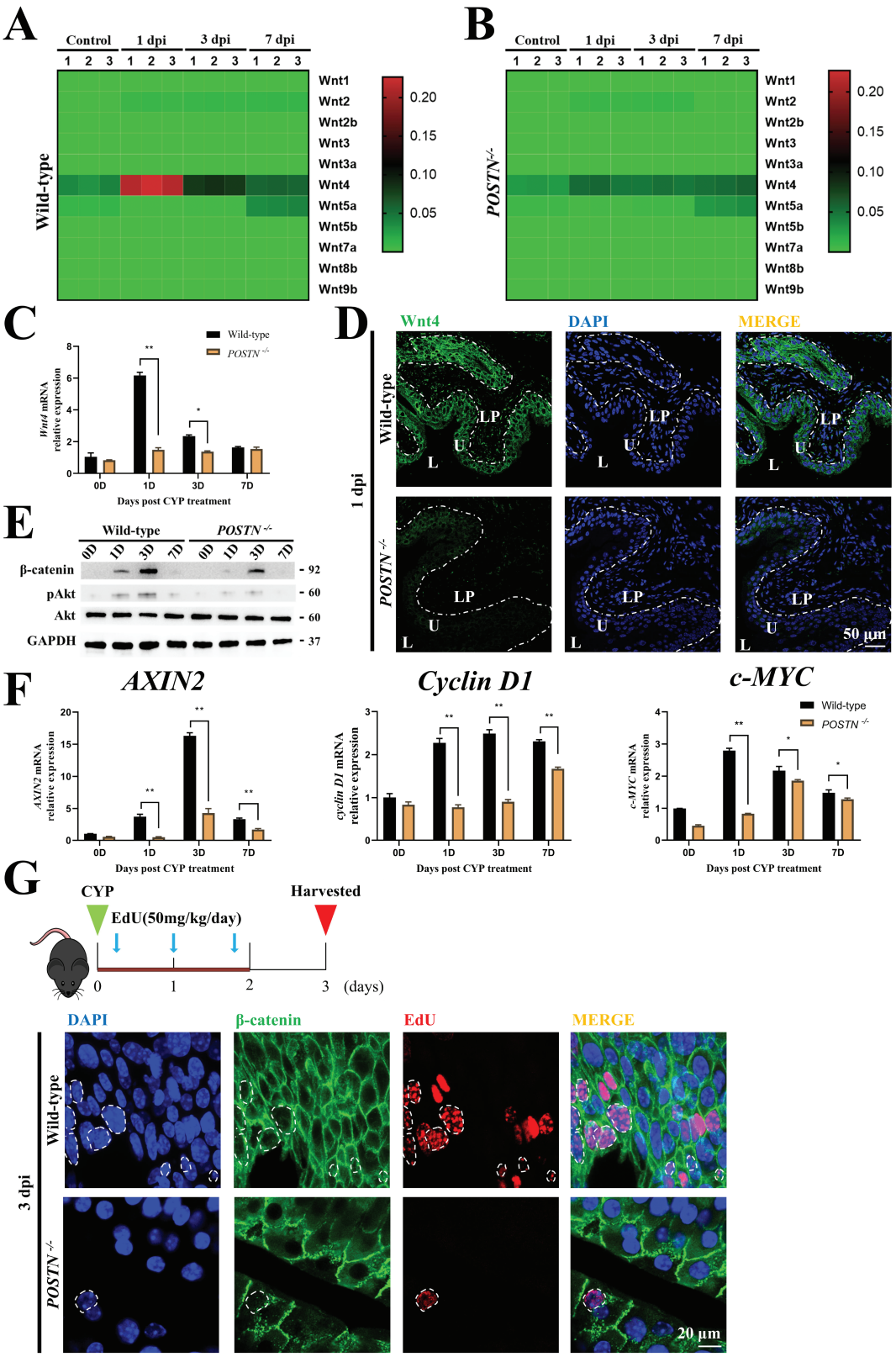

Figure 5. Periostin upregulates Wnt4 expression and activates AKT/β-catenin signaling. (**A-B**) Heat map depiction of Wnt ligands in bladders of wild-type and *POSTN*$^{-/-}$mice after CYP treatment. (**C**) qRT-PCR analysis of Wnt4 mRNA expression level in bladders of both groups. (**D**) Immunostaining showing expression of Wnt4 in bladders of both groups. (**E**) Western blots of β-catenin, pAKT, AKT, and GAPDH, showing decreased protein levels of β-catenin and pAKT in POSTN deficient mice. (**F**) The qRT-PCR analysis of β-catenin targeted genes (*C-MYC, AXIN2,* and *Cyclin D1*) in CYP–treated bladders of both groups. (G) Immunofluorescent staining for β-catenin (green) and EdU (red). Dotted circles indicate nuclear translocation of β-catenin in EdU–incorporating urothelial cells. All data were represented as mean ± SEM. Unpaired Student's *t*-test, **P* < .05, and ***P* < .01, *POSTN*$^{-/-}$ group versus wild–type group.

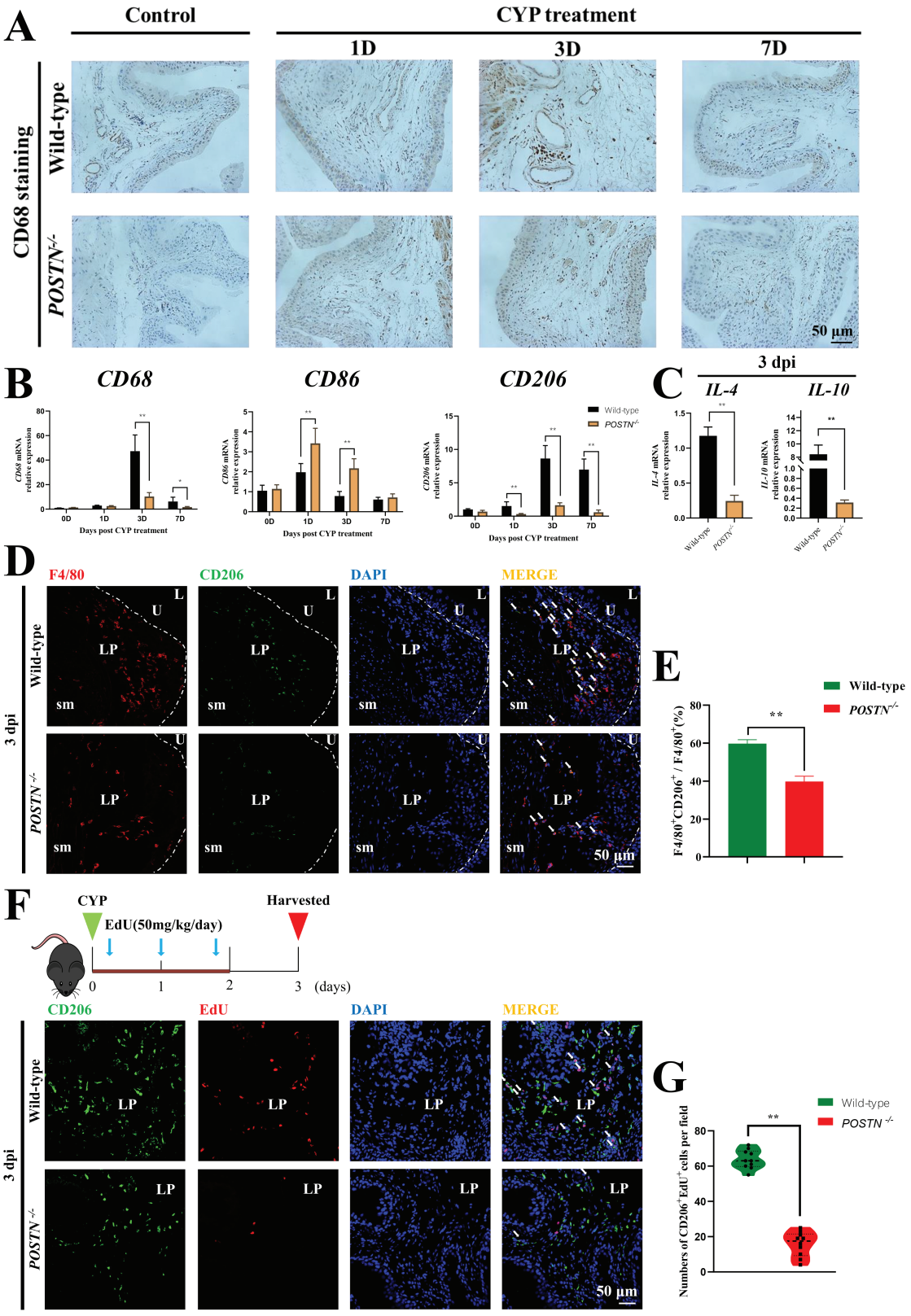

Figure 6. Periostin promotes resident macrophages proliferation and polarization to the M2-subtype. (**A**) Immunohistochemical staining for CD68 (a marker of pan-macrophage) in bladder cross-sections of wild-type and *POSTN*$^{-/-}$ mice at indicated days post–CYP treatment. (**B**) The qRT-PCR analysis showed that expression of *CD68* (pan-macrophage), *CD86* (M1 macrophage), and *CD206* (M2 macrophage) in bladders at indicated days (0, 1, 3, 7 days post–CYP treatment). (**C**) The qRT-PCR analysis showed that expression of M2 macrophage secreted pro–regenerative cytokines, IL4, and IL10, in bladders of both groups 3 days after CYP treatment. (**D**) Immunofluorescent co-staining of F4/80 (red) and CD206 (green) in bladder cross-sections on day 3 post–CYP treatment. Scale bar, 50 μm. (**E**) Quantitative analysis showing the proportion of F4/80^{+}CD206^{+} M2 macrophages in F4/80^{+} pan-macrophages. (**F**) Immunofluorescent co-staining of EdU (red) and CD206 (green) in bladder cross-sections at day 3 post–CYP treatment. Scale bar, 50 μm. (**G**) Quantitative analysis showing the number of CD206/EdU double-positive macrophages, indicating proliferative resident macrophages. All data were represented as mean ± SEM. Unpaired Student's *t*-test, **P* < .05, and ***P* < .01, *POSTN*$^{-/-}$ group versus wild–type group.

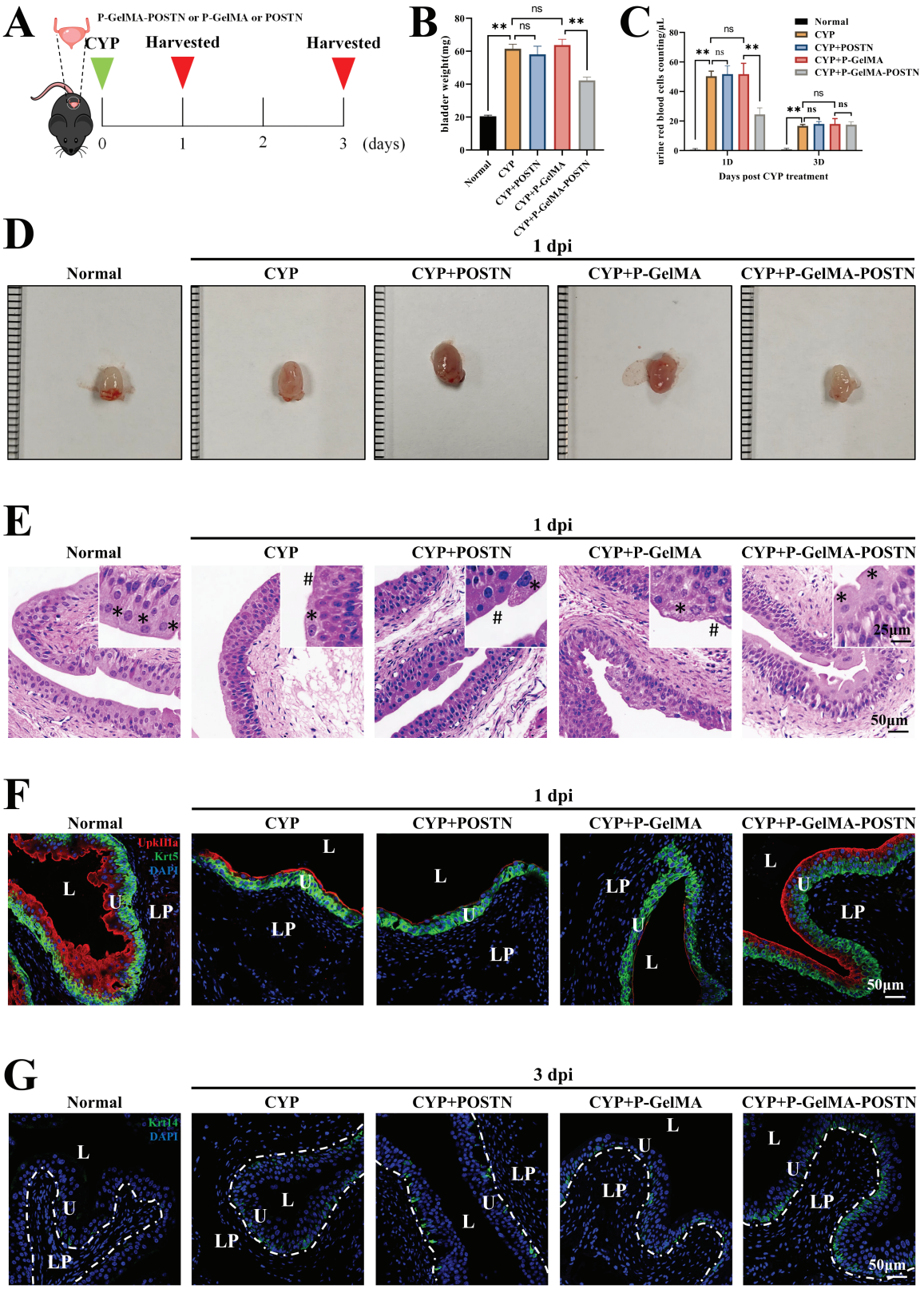

Figure 7. Intravesical administration of P-GelMA–loaded recombinant Periostin accelerates urothelial regeneration after CYP–induced bladder injury. (**A**) Schematic depiction of the experimental procedure used for intravesical administration of POSTN, P-GelMA, and P-GelMA–loaded with POSTN immediately post–CYP injection. (**B**) Weights of the bladder were assessed in each group 1 day after CYP administration. (**C**) The number of urine red blood cells was counted in both groups 1 and 3 days after CYP treatment. (**D**) Appearance of bladders in each group 1 day post–CYP treatment. (**E**) Representative images show H&E staining of bladder cross-sections in each group. * and # indicate the presence or the absence of superficial umbrella cells, respectively. (**F**) Co-staining for UpkIIIa (red) and Krt5 (green) in bladder cross-sections of indicated group 1 day post–CYP treatment. Scale bar, 50 μm. (**G**) Immunostaining showing Krt14 labeled urothelial stem cells in each group.

Urothelial regeneration requires signals from both stroma and urothelium, including BMP4, Wnt signaling pathway, Delta-Notch, sonic Hedgehog, TP63, and various growth factors.[12,38-41] Here, we used a CYP-induced acute cystitis mouse model to study mechanisms underlying urothelial injury and regeneration and verified that POSTN mediated a crosstalk between stroma and urothelium in the bladder and contributed to urothelial regeneration. Mice lacking POSTN exhibited more severe hematuria after CYP treatment and worsen bladder structure, such as suburothelial edema, umbrella cells exfoliation, and inflammatory cells infiltration. The superficial umbrella cell layer is extremely important for the maintenance of the blood–urine barrier, as it is the only cell layer of the urothelium that forms identifiable tight junctions, adherence junctions, and specialized regions of cellular contact.[8,42,43] We, therefore, detected the loss and recovery of umbrella cells and found that Krt20 or UpkIIIa labeled umbrella cells recovered much slower in POSTN KO mice. Besides, POSTN deficiency disturbed the expression of uroplakins and tight junction and adherence junction proteins, such as *ZO-1*, *OCLD,* and *Cdh1*, indicating a delayed recovery of umbrella cells and blood–urine barrier.

Renewal of damaged urothelium is considered as the core mechanism of urothelial regeneration. When umbrella cells are removed by chemical injury or bacterial infection, it triggers a dramatic upregulation in urothelial proliferation. Previous studies revealed that Krt5$^+$ and SHH$^+$ basal cells served as potential urothelial progenitor cells to proliferate and give rise to other cell types in the urothelium.[10,12,38] More recently, Papafotiou et al. revealed that Krt14 distinguished a subpopulation of Krt5$^+$ and SHH$^+$ basal cells as urothelial stem cells.[9] We observed a dramatic increase of pHH3$^+$ and Ki67$^+$ proliferative urothelial cells post–CYP treatment, whereas POSTN deficiency diminished the proliferative response of urothelium. By tracing EdU-labeled urothelial cells 3 days post-injury, we found a higher number of EdU-incorporating urothelial cells in wild–type mice than that in *POSTN*$^{-/-}$ mice, and these EdU positive cells were co-stained with Krt5$^+$ basal cells and UpkIIIa$^+$ umbrella cells. Besides, Western blot and immunofluorescence showed a downregulated expression of Krt14, a marker of urothelial stem cells, in POSTN deficient mice. Taken together, these results demonstrated that POSTN deficiency disturbed basal cells or urothelial stem cells proliferation and thus delayed urothelial regeneration.

The Wnt/β-catenin pathway is essential for promoting urothelial proliferation and differentiation. In response to acute injury, Shh secreted by basal cells increased and upregulated expression of Wnt ligands in stromal cells, which in turn stimulated urothelial proliferation and regeneration.[12] Besides, POSTN secreted by cancer-associated fibroblast can recruit Wnt ligands and thereby increase Wnt signaling in cancer stem cells.[44] In this study, we screened various Wnt ligands and found expression of Wnt4 is highly upregulated in CYP–injured bladder of wild–type mice rather than *POSTN*$^{-/-}$ mice. Subsequently, expression levels of β-catenin elevated and peaked at day 3 post-injury, and a higher level was detected in wild–type mice than that in *POSTN*$^{-/-}$ mice. Moreover, nuclear translocation of β-catenin was observed and mainly co-expressed with EdU-incorporating urothelial cells, indicating an activation of Wnt/β-catenin signaling and subsequent induction of related genes (*c-Myc, CCND1*, and *AXIN2*) in wild–type mice. In addition, POSTN can also activate the Akt pathway, which can decrease the activity level of glycogen synthase kinase-3β (GSK3β) and thus prevent β-catenin from degradation. In summary, POSTN can upregulate Wnt4 expression in the bladder and activate AKT signaling in the urothelium, which together activates β-catenin signaling and thus promotes urothelial proliferation.

Macrophages contribute to tissue regeneration, repair, and remodeling in various tissues.[45,46] Upon injury, inflammatory monocytes selectively traffic to the damaged tissue and then be locally differentiated toward a proinflammatory macrophage known as M1 subtype, or a pro–regenerative macrophage known as M2 subtype in response to microenvironmental factors. Periostin can directly regulate macrophages in several aspects, including macrophage recruitment, proliferation, and polarization.[15,19,20,47] Our results show that a less abundance of CD68$^+$ pan-macrophages was observed in the CYP–injured bladder of POSTN–deficient mice. This decrease was partially associated with the POSTN promotes resident macrophage proliferation, as we observed a lower number of CD206/EdU$^+$ in *POSTN*$^{-/-}$ mice compared to wild–type mice. More importantly, although a lower expression level of CD68 was detected by qRT-PCR in *POSTN*$^{-/-}$ mice, a higher expression of *CD86* (M1 marker) and lower CD206 (M2 marker) were also assessed compared to wild–type mice, indicating that POSTN promotes macrophage polarization to M2 subtype. Furthermore, the proportion of F4/80$^+$CD206$^+$macrophages is lower in the bladder of *POSTN*$^{-/-}$ mice at day 3 post–CYP administration, and transcriptions of pro–regenerative cytokines such as *IL-4* and *IL-10* were much less compared to wild–type mice. Taken together, we conclude that POSTN can induce macrophage proliferation and polarization into the M2 phenotype, thus providing a pro–regenerative microenvironment for urothelial regeneration.

We have so far demonstrated that POSTN played an important role in urothelial regeneration, and could serve as a therapeutic target for bladder diseases. However, we found that intravesical delivery of recombinant POSTN solution could not alleviate CYP–induced bladder injury, most likely because of a rapid elimination of POSTN by urination. Biomaterial carriers have been reported as a promising strategy for intravesical drug delivery, which can prevent premature drug release by urine, prolong the drug retention time and diminish the undesired systemic side-effects.[27] Therefore, we used P-GelMA to load recombinant POSTN and found that intravesical delivery of P-GelMA–loaded POSTN could promote urothelial regeneration, decrease umbrella cells exfoliation and hence alleviate hematuria. Even though CYP–induced interstitial cystitis in a mouse model is not as severe as that in a rat model, we have preliminary proved the efficacy of POSTN in the treatments of interstitial cystitis. To some extent, POSTN is a promising bioactive molecule in urothelial regeneration, and its combination with biomaterials could be a potential target for bladder injury and repair or even tissue–engineered bladder.

Conclusions

Our results demonstrate a novel and pivotal role of POSTN in bladder urothelial regeneration post–CYP-induced injury. Upon acute injury, umbrella cells exfoliation triggers upregulation of POSTN in the stroma, and in return, stroma secreted POSTN drives urothelial stem cells proliferation and differentiation into umbrella cells, namely

urothelial regeneration. Periostin mediated urothelium–stroma interaction contains at least 2 mechanisms: (1) POSTN promotes basal cells or urothelial stem cell proliferation and restores damaged umbrella cells by induction of Wnt4/AKT/β-catenin signaling, and (2) POSTN induces resident macrophage proliferation and polarization into a pro–regenerative phenotype, thus favoring urothelial regeneration. Furthermore, we develop a novel treatment for interstitial cystitis by intravesical administration of P-GelMA granular hydrogel–loaded recombinant POSTN, which is expected to achieve clinical application and benefit patients with cystitis.

Acknowledgments

We would like to thank Mrs. Yuanjun Guan for the assistance in the performance of the confocal microscope.

Funding

This work was supported by the National Key Research and Development Program of China (2017YFA0103802, M.H.J.); the National Natural Science Foundation of China (31972894, 81770290, M.H.J., 81671449, 81971314, C.D.); the Science and Technology Planning Project of Guangdong Province (2016B030229006, 2014A020211007, M.H.J., 2016B030230001, C.D.); the Key Scientific and Technological Program of Guangzhou City (201604020158, M.H.J., 201604020189, C.D.); the Key Program of Natural Science Foundation of Guangdong Province (2018B030311039, C.D.).

Conflict of Interest

The authors declared no potential conflicts of interest with respect to the research, authorship, and/or publication of this article.

Author Contributions

J.M.H. and D.C.H.: conceived and designed the study and revised the manuscript. C.Z.H., L.L.Y., and C.Y.H.: performed most of the experiments and wrote the manuscript. L.M.J.: helped to collect the data. X.A.P.: helped to revise the manuscript. All authors read and approved the final manuscript.

Data Availability

All data generated or analyzed during this study are included in this published article [and its supplementary information files].

Supplementary Material

Supplementary material is available at *Stem Cells Translational Medicine* online.

References

1. Jensen MM, Jia W, Schults AJ, et al. Temperature-responsive silk-elastinlike protein polymer enhancement of intravesical drug delivery of a therapeutic glycosaminoglycan for treatment of interstitial cystitis/painful bladder syndrome. *Biomaterials*. 2019;217:119293.
2. Clemens JQ, Mullins C, Ackerman AL, et al. Urologic chronic pelvic pain syndrome: insights from the MAPP Research Network. *Nat Rev Urol*. 2019;16(3):187-200.
3. Nickel JC, Herschorn S, Whitmore KE, et al. Pentosan polysulfate sodium for treatment of interstitial cystitis/bladder pain syndrome: insights from a randomized, double-blind, placebo controlled study. *J Urol*. 2015;193(3):857-862.
4. Birder LA. Pathophysiology of interstitial cystitis. *Int J Urol*. 2019;26(Suppl 1):12-15.
5. Dalghi MG, Montalbetti N, Carattino MD, et al. The urothelium: life in a liquid environment. *Physiol Rev*. 2020;100(4):1621-1705.
6. Kreft ME, Hudoklin S, Jezernik K, et al. Formation and maintenance of blood-urine barrier in urothelium. *Protoplasma* 2010;246(1-4):3-14.
7. Sun TT, Zhao H, Provet J, et al. Formation of asymmetric unit membrane during urothelial differentiation. *Mol Biol Rep*. 1996;23(1):3-11.
8. Carattino MD, Prakasam HS, Ruiz WG, et al. Bladder filling and voiding affect umbrella cell tight junction organization and function. *Am J Physiol Renal Physiol*. 2013;305(8):F1158-F1168.
9. Papafotiou G, Paraskevopoulou V, Vasilaki E, et al. KRT14 marks a subpopulation of bladder basal cells with pivotal role in regeneration and tumorigenesis. *Nat Commun*. 2016;7:11914.
10. Colopy SA, Bjorling DE, Mulligan WA, et al. A population of progenitor cells in the basal and intermediate layers of the murine bladder urothelium contributes to urothelial development and regeneration. *Dev Dyn*. 2014;243(8):988-998.
11. Wang C, Ross WT, Mysorekar IU. Urothelial generation and regeneration in development, injury, and cancer. *Dev Dyn*. 2017;246(4):336-343.
12. Shin K, Lee J, Guo N, et al. Hedgehog/Wnt feedback supports regenerative proliferation of epithelial stem cells in bladder. *Nature* 2011;472(7341):110-114.
13. Horiuchi K, Amizuka N, Takeshita S, et al. Identification and characterization of a novel protein, periostin, with restricted expression to periosteum and periodontal ligament and increased expression by transforming growth factor beta. *J Bone Miner Res Off J Am Soc Bone Mineral Res*. 1999;14(7):1239-1249.
14. Wang Y, Jin S, Luo D, et al. Functional regeneration and repair of tendons using biomimetic scaffolds loaded with recombinant periostin. *Nat Commun*. 2021;12(1):1293.
15. Kormann R, Kavvadas P, Placier S, et al. Periostin promotes cell proliferation and macrophage polarization to drive repair after AKI. *J Am Soc Nephrol*. 2019;31(1):85-100.
16. Chen Z, Xie J, Hao H, et al. Ablation of periostin inhibits post-infarction myocardial regeneration in neonatal mice mediated by the phosphatidylinositol 3 kinase/glycogen synthase kinase 3beta/cyclin D1 signalling pathway. *Cardiovasc Res*. 2017;113(6):620-632.
17. Wu T, Huang J, Wu S, et al. Deficiency of periostin impairs liver regeneration in mice after partial hepatectomy. *Matrix Biol*. 2018;66:81-92.
18. Smid JK, Faulkes S, Rudnicki MA. Periostin induces pancreatic regeneration. *Endocrinology*. 2015;156(3):824-836.
19. Allard DE, Wang Y, Li JJ, et al. Schwann cell-derived periostin promotes autoimmune peripheral polyneuropathy via macrophage recruitment. *J Clin Invest*. 2018;128(10):4727-4741.
20. Liao Y, Li G, Zhang X, et al. Cardiac nestin(+) mesenchymal stromal cells enhance healing of ischemic heart through periostin-mediated M2 macrophage polarization. *Mol Ther*. 2020;28(3):855-873.
21. Guo C, Balsara ZR, Hill WG, et al. Stage- and subunit-specific functions of polycomb repressive complex 2 in bladder urothelial formation and regeneration. *Development (Cambridge, England)*. 2017;144(3):400-408.
22. Zhang X, Gao S, Tanaka M, et al. Carbenoxolone inhibits TRPV4 channel-initiated oxidative urothelial injury and ameliorates cyclophosphamide-induced bladder dysfunction. *J Cell Mol Med*. 2017;21(9):1791-1802.

23. Chung S, Kang D-O, Yamzon J, et al. O-GlcNAc mediated glycosylation down-regulation in mice with cyclophosphamide induced cystitis. *J Urol*. 2010;183(1):351-356.
24. Liu S, Jin M, Chen Y, et al. High internal phase emulsions stabilised by supramolecular cellulose nanocrystals and their application as cell-adhesive macroporous hydrogel monoliths. *J Mater Chem B*. 2017;5(14):2671-2678.
25. Xu M, Li Q, Fang Z, et al. Conductive and antimicrobial macroporous nanocomposite hydrogels generated from air-in-water Pickering emulsions for neural stem cell differentiation and skin wound healing. *Biomater Sci*. 2020;8(24):6957-6968.
26. Liu S, Qi D, Chen Y, et al. Quadruple hydrogen bonds and thermo-triggered hydrophobic interactions generate dynamic hydrogels to modulate transplanted cell retention. *Biomater Sci*. 2019;7(4):1286-1298.
27. Lin Z, Hu H, Liu B, et al. Biomaterial-assisted drug delivery for interstitial cystitis/bladder pain syndrome treatment. *J Mater Chem B*. 2021;9(1):23-34.
28. Chen Z, Xie J, Hao H, et al. Ablation of periostin inhibits post-infarction myocardial regeneration in neonatal mice mediated by the phosphatidylinositol 3 kinase/glycogen synthase kinase 3β/cyclin D1 signalling pathway. *Cardiovasc Res*. 2017;113(6):620-632.
29. Hausmann S, Regel I, Steiger K, et al. Loss of periostin results in impaired regeneration and pancreatic atrophy after cerulein-induced pancreatitis. *Am J Pathol*. 2016;186(1):24-31.
30. Duchamp de Lageneste O, Julien A, Abou-Khalil R, et al. Periosteum contains skeletal stem cells with high bone regenerative potential controlled by Periostin. *Nat Commun*. 2018;9(1):773.
31. Jost SP. Cell cycle of normal bladder urothelium in developing and adult mice. *Virchows Arch B Cell Pathol Incl Mol Pathol*. 1989;57(1):27-36.
32. Jost SP, Potten CS. Urothelial proliferation in growing mice. *Cell Tissue Kinetics*. 1986;19(2):155-160.
33. Balsara ZR, Li X. Sleeping beauty: awakening urothelium from its slumber. *Am J Physiol Renal Physiol*. 2017;312(4):F732-F743.
34. Erman A, Jezernik K, Stiblar-Martincic D, et al. Postnatal restoration of the mouse urinary bladder urothelium. *Histochem Cell Biol*. 2001;115(4):309-316.
35. Erman A, Kerec Kos M, Zakelj S, et al. Correlative study of functional and structural regeneration of urothelium after chitosan-induced injury. *Histochem Cell Biol*. 2013;140(5):521-31.
36. Gandhi D, Molotkov A, Batourina E, et al. Retinoid signaling in progenitors controls specification and regeneration of the urothelium. *Dev Cell*. 2013;26(5):469-482.
37. Peyton CC, Burmeister D, Petersen B, et al. Characterization of the early proliferative response of the rodent bladder to subtotal cystectomy: a unique model of mammalian organ regeneration. *PLoS One*. 2012;7(10):e47414.
38. Mysorekar IU, Isaacson-Schmid M, Walker JN, et al. Bone morphogenetic protein 4 signaling regulates epithelial renewal in the urinary tract in response to uropathogenic infection. *Cell Host Microbe*. 2009;5(5):463-475.
39. Mysorekar IU, Mulvey MA, Hultgren SJ, et al. Molecular regulation of urothelial renewal and host defenses during infection with uropathogenic Escherichia coli. *J Biol Chem*. 2002;277(9):7412-7419.
40. Pignon JC, Grisanzio C, Geng Y, et al. p63-expressing cells are the stem cells of developing prostate, bladder, and colorectal epithelia. *Proc Natl Acad Sci USA*. 2013;110(20):8105-8110.
41. de Boer WI, Schuller AG, Vermey M, et al. Expression of growth factors and receptors during specific phases in regenerating urothelium after acute injury in vivo. *Am J Pathol*. 1994;145(5):1199-1207.
42. Acharya P, Beckel J, Ruiz WG, et al. Distribution of the tight junction proteins ZO-1, occludin, and claudin-4, -8, and -12 in bladder epithelium. *Am J Physiol Renal Physiol*. 2004;287(2):F305-F318.
43. Wang J, Batourina E, Schneider K, et al. Polyploid superficial cells that maintain the urothelial barrier are produced via incomplete cytokinesis and endoreplication. *Cell Rep*. 2018;25(2):464-477.e4.
44. Yu B, Wu K, Wang X, et al. Periostin secreted by cancer-associated fibroblasts promotes cancer stemness in head and neck cancer by activating protein tyrosine kinase 7. *Cell Death Dis*. 2018;9(11):1082.
45. Wynn TA, Chawla A, Pollard JW. Macrophage biology in development, homeostasis and disease. *Nature*. 2013;496(7446):445-455.
46. Wynn TA, Vannella KM. Macrophages in tissue repair, regeneration, and fibrosis. *Immunity*. 2016;44(3):450-462.
47. Zhou W, Ke SQ, Huang Z, et al. Periostin secreted by glioblastoma stem cells recruits M2 tumour-associated macrophages and promotes malignant growth. *Nat Cell Biol*. 2015;17(2):170-182.